Channel bonding transceivers for efficient 100 Gb/s and beyond wireless and plastic wave guide communications

J L González-Jiménez, A. Siligaris, A. Hamani, C. Dehos, F. Foglia Manzillo, A. Clemente, N. Cassiau

Channel Bonding Transceivers for Efficient 100 Gb/s and Beyond Wireless and Plastic Waveguide Communications

J.L. González-Jiménez, A. Siligaris, A. Hamani, C. Dehos, F. Foglia Manzillo, A. Clemente, N. Cassiau
Université Grenoble-Alpes, CEA-Leti, F-38000 Grenoble, France

***Abstract*—High-data rate communications in the range of 100 Gbps require handling larger RF bandwidths in frequency bands beyond 100 GHz. The architecture of the transceiver should be reconsidered compared with classical approaches in order to optimize the power consumption. Channel bonding architectures combine relatively low baseband bandwidth inputs with power combining and up-conversion stages in order to obtain a large bandwidth at RF. In this paper, some implementations of energy efficient transceivers using this operating principle at D-band (around 140 GHz) will be presented. Wireless communications and plastic waveguide links are demonstrated with data rates of several tens of Gbps and energy consumption in the order of a few tens of pJ/bit.**

Keywords—D-band, channel bonding, high data-rate, wireless point-to-point links, plastic waveguide links

I. INTRODUCTION

The current trend towards increasing communication data rates (DR) driven by the requirements of 5G and future 6G networks, among others, is pushing the transceivers towards ultra-broadband architectures and the carrier frequencies towards higher frequencies in the mmW and sub-THz spectrum, such as the D-band, in the quest of more available bandwidth (BW). It has been recently shown that channel capacity as defined by Shannon's theorem peaks for moderately complex modulations such as 16-QAM or 64-QAM [1]. Therefore, in order to attain 100 Gb/s and higher DR, channel BW in the order of a few tens of GHz is required. Handling this BW from the baseband (BB) to the RF is really challenging and usually requires high power consumption. An alternative is to address separately the total required band by using channel-bonding architectures. The basic principle is shown in Fig.1 and a transmitter (TX) implementation example is shown in Fig. 2. It allows reducing the BW of the BB interfaces and the fractional BW of most of the RF up-conversion circuitry. The first channel-bonding and up-conversion step in this example is implemented by a multi-channel circuit operating at V-band band and the second channel-bonding step is implemented by a D-band multi-channel up-converter, as illustrated in Fig. 2.

II. CHANNEL BONDING ARCHITECTURES

A. Impact on digital interfaces energy efficiency

The benefits of a low baseband bandwidth in terms of energy efficiency becomes clear when analyzing the figure of merit reported by B. Murmann [2] in his survey of data converters shown in Fig. 3. This figure shows that for sampling rates beyond a few hundreds of MHz, the energy consumption per conversion stage ($FOM_{W,hf}$) increases exponentially with the sampling rate (f_{snyq}). Consider that a total RF BW of e.g. 5 GHz is required to achieve a given

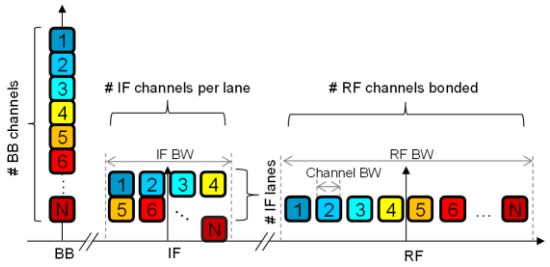

Fig. 1 Frequency plan for channel bonding architectures.

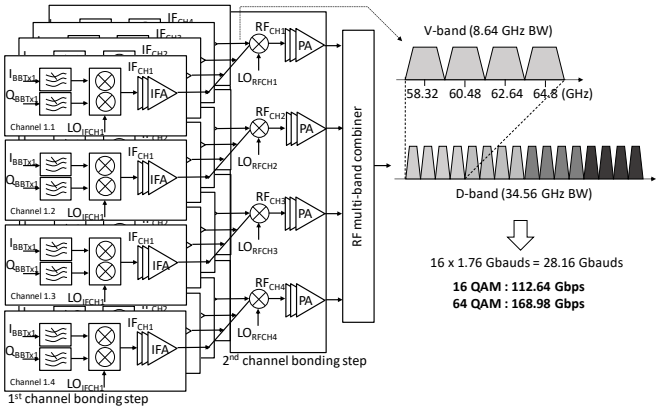

Fig. 2 Ultra broadband channel bonding TX architecture.

data-rate. The signal at RF can come from a single BB channel with 5 GHz of BW or from two BB channels with 2.5 GHz of BW each. The figure tells us that the second option will be much energy efficient since two data converters with a sampling rate of 5 GS/s would consume less than a single 10 GS/s data converter.

B. Power combining approaches

Another important aspect of channel bonding architectures is the technique used for bonding together the

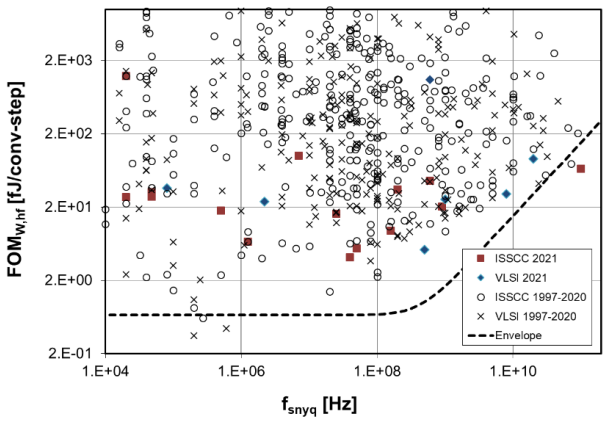

Fig. 3 Energy consumption vs sampling rate of data converters from [1]

different channels processed in parallel by the various transmitter or receiver lanes. This can be accomplished by current combining techniques such as in [3] or by passive integrated combiners like [4]. However, passive combiner at high frequencies usually introduce significant insertion losses. An alternative is to co-design the receiver and transmitter integrated circuits along with the antennas in order to implement over-the-air multi-band power combining. The benefits of this approach are illustrated in Fig. 4 that shows an experimental comparison of the EIRP obtained from the same TX IC implementing the two highest frequency D-band up-conversion lanes of Fig. 1. In the first case, the two sub-bands are bonded using an in-package surface integrated waveguide (SIW) passive combiner and then feed to a four-patch antenna [5]. In the second case, each band is radiated by one-half of a similar patch array antenna and combined over-the-air [6]. Even though the antenna gain per sub-band is halved in this second case, the elimination of the insertion losses of the in-package combiner allows increasing by 9 dB the EIRP.

C. *Multiple Local Oscillator Signals Generation*

The up and down conversion of multiple BB channels to/from RF requires multiple and simultaneous LO signals. Instead of using a dedicated PLL for each LO frequency, high-order integer N frequency multiplication can be used to generate several LO frequencies at multiples of a common reference signal frequency. The operation principle is illustrated in Fig. 5. The reference input signal is used for periodically and coherently switch on and off an oscillator. This produces a signal with harmonic terms at integer multiples of that reference input signal frequency. One particular harmonic term can then be selected using a couple of cascaded injection locked oscillators. In order to generate multiple LO signals, several copies of the same circuit each tuned to select a different harmonic terms (N, N+1, N+2, etc.) of the multi-harmonic pulsed oscillator signal can be used, as demonstrated in [7] and shown in Fig. 6. The reference frequency sets the LO spacing. The four LO signals shown in the figure are the ones required in the first up-conversion stage of the channel-bonding architecture of Fig. 2

III. IMPLEMENTATION EXAMPLES

The applications of channel bonding architectures to high-data rate communication are illustrated in this section with two examples, one corresponding to a point-to-pint link and another one for plastic waveguide communications.

A. *D-band point-to-point link*

A first hardware realization of the highest frequency section of the second channel-bonding step shown in Fig. 2 is shown in Fig. 7. It combines a couple of integrated circuits (ICs) implemented in 45nm SOI technology a multi-channel transmitter and receiver (RX), respectively, and an antenna-in-package realizing over-the-air power combining/splitting. The TX IC is composed of two up-conversion lanes including an intermediate frequency (IF) amplifier, mixer and power amplifier (PA) for each of the lanes. The same IF input is re-used for the two up-conversion lanes for testing purposes, but in a final implementation each lane would have its separate IF input signal. The RX IC integrates also two down-conversion lanes each composed of an LNA, a mixer and IF amplifier. The two LO required at the TX and RX ICs are generated on-chip using the technique outlined in section

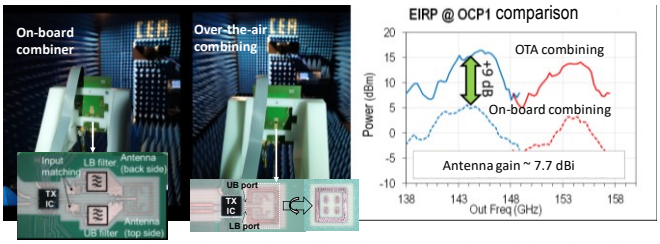

Fig. 4 Comparison of two alternatives for mmW channel bonding: in-pagckage *vs* over-the-air (OTA) power combining.

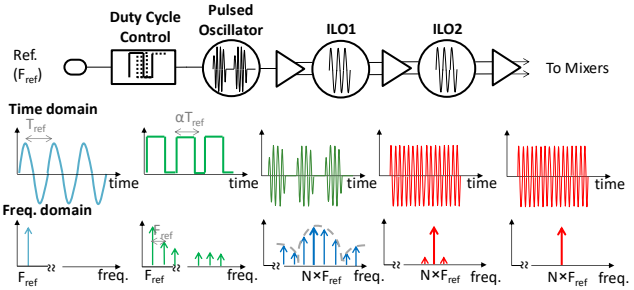

Fig. 5 Multiple LO generation operation principle.

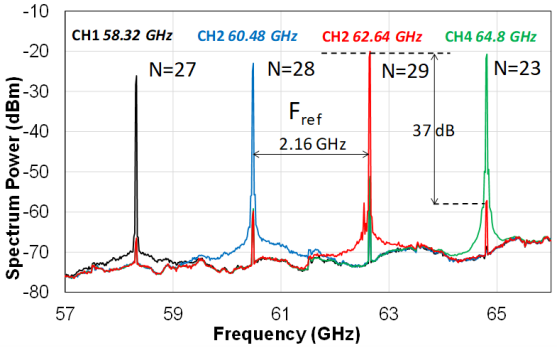

Fig. 6 Experimental demonstration of multi-LO generation form [7].

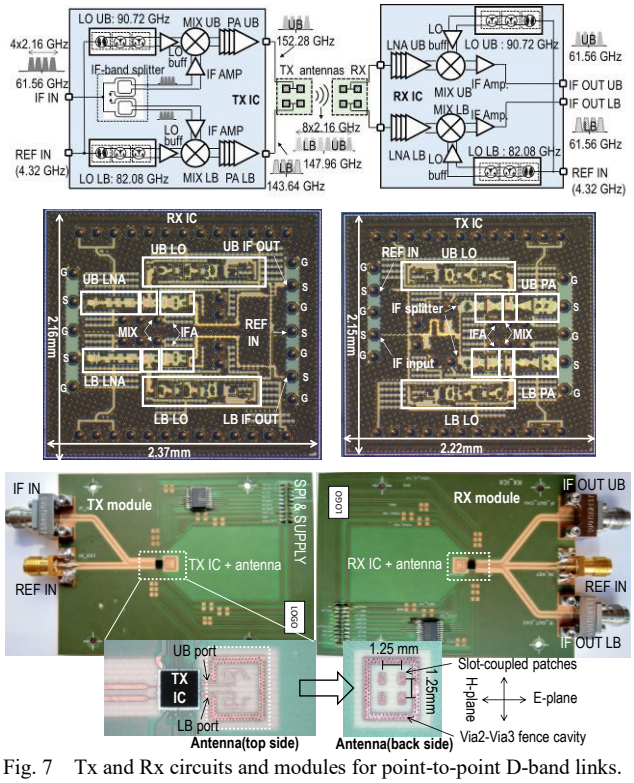

Fig. 7 Tx and Rx circuits and modules for point-to-point D-band links.

II.C. The IF BW handled by each TX or RX lane is limited to 8.64 GHz, centered at the V-band (61.56 GHz) as illustrated in Fig. 2 and in the block diagrams of Fig. 7. The PAs of the TX and the LNAs of the RX have also a relaxed BW constraint since they only handle a portion of the D-band signal in the frequency domain. Their schematics are shown in Fig. 8. The only element that covers the full band is the in-package antenna. The two modules shown in Fig. 7 are mounted in a point-to-point link hardware-in-the-loop (HIL) demonstration platform, as shown in Fig. 9.

The TX module is extended with an electromagnetic planar lens based in a transmit array (TA) implemented with low-cost PCB technology [5]. It allows boosting the emitted power by 20 dB in comparison to the EIRP shown in Fig. 4. The TX IF signal is generated using a large-band arbitrary waveform generator (AWG) that outputs a multi-channel baseband (BB) signal, and an external up-conversion mixer. The TX module radiates a signal at D-band composed of eight BB channels, each one carrying 1.76 Gbauds of modulated signal. The RX receives and down-converts this signal to IF, providing two separate IF outputs that are sampled using a digital sampling oscilloscope (DSO). The samples are next processed by a digital BB RX implemented in Matlab that demodulates each of the channels of which the RF signal is composed and calculates performance metrics such as EVM and BER.

This point to point D-band link has been recently demonstrated in [6] featuring 56.32 Gb/s at 2 cm (without the TA) with BER of 10^{-3} on each of the 8 channels of which the D-band signal is composed, each carrying a 16-QAM single carrier modulated signal. The TA on the TX side ads 20 dB to the link budget, extending the range to 20 cm. By adding the same TA at the RX side, the link would be able to attain 2 m of range. The power consumption of the TX and RX circuits are 600 mW and 400 mW, respectively, resulting in an energy efficiency for the link of 18 pJ/b. The circuits are able also to carry a 64-QAM modulated signal as shown in Fig. 10, with a reduced range or channel BW.

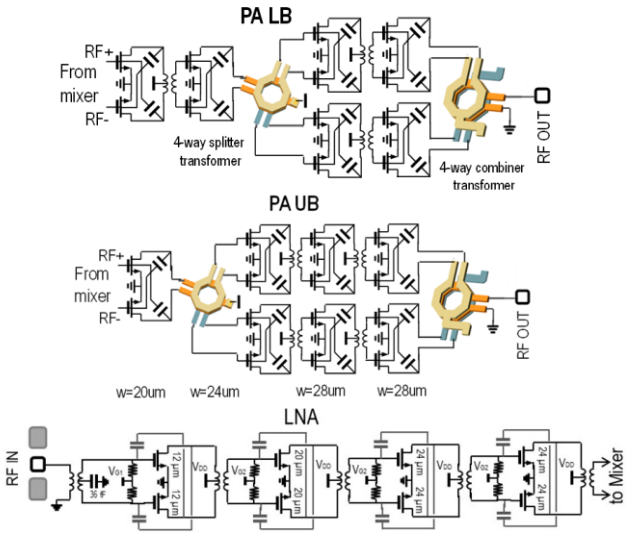

Fig. 8. D-band PAs and LNA circuits schematic.

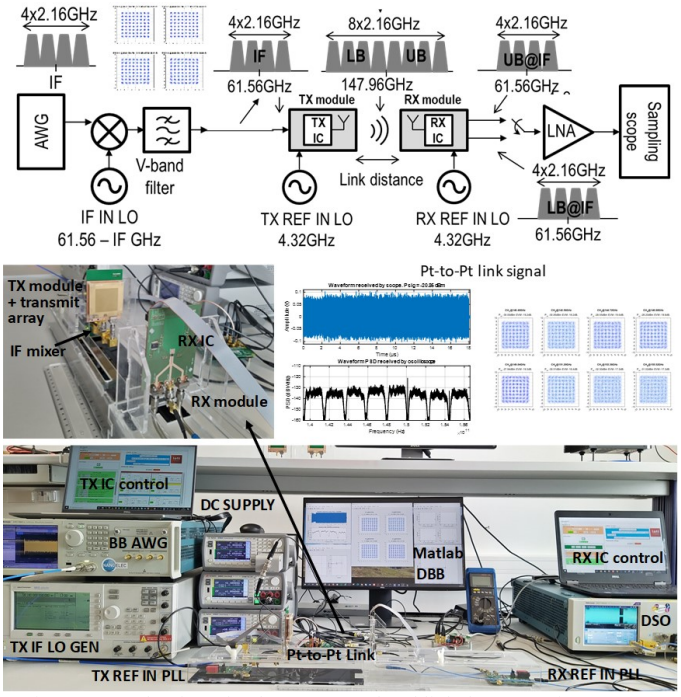

Fig. 9 HIL platefrom for the pt-to-pt D-band link demonstration.

B. *Plastic waveguide communications*

Channel aggregation is also an efficient way to adapt to the specific characteristics of plastic waveguide mmW links such as long group delay and frequency dependent losses. By subdividing the full signal band in smaller channels, each one can carry the most suitable modulation as a function of the link quality. The same TX IC presented in the previous section is combined with an in package SIW diplexer (the same shown in Fig.4) and a WR6.5 SIW transition to feed a plastic waveguide as shown in Fig. 11. The RX is implemented using a commercial D-band receiver with a custom-made fiber holder in front of the RX WR6.5 waveguide flange. The plastic waveguide is a PTF hollowed cylinder with 2 mm external diameter and 1 mm internal dimeter and has optimal dimensions to operate at the D-band. The fiber losses have been experimentally characterized and they vary from ra 2.9 dB/m at 110 GHz up to 7.6 dB/m at 170 GHz Different lengths form 1 m to 4 m has been tested and reported in [8]. Thanks to the channel bonding architecture, adaptive modulation can be used at each channel depending on the propagation characteristics. This allows adapting the modulation scheme and achieve the best possible overall data-rate as shown in Fig. 12.

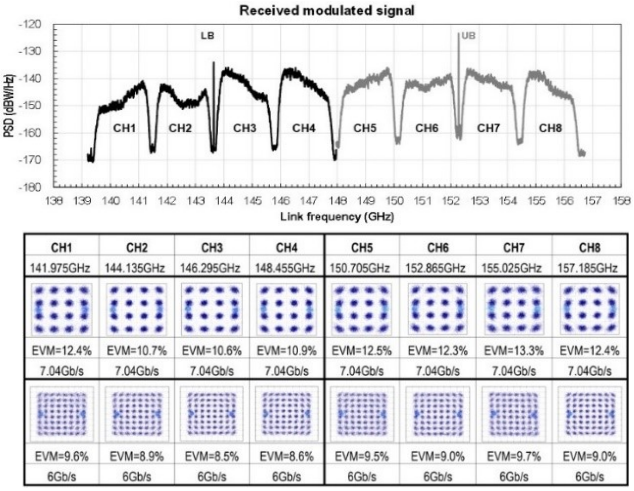

Fig. 10 D-band wireless link signal and demodulated constellations.

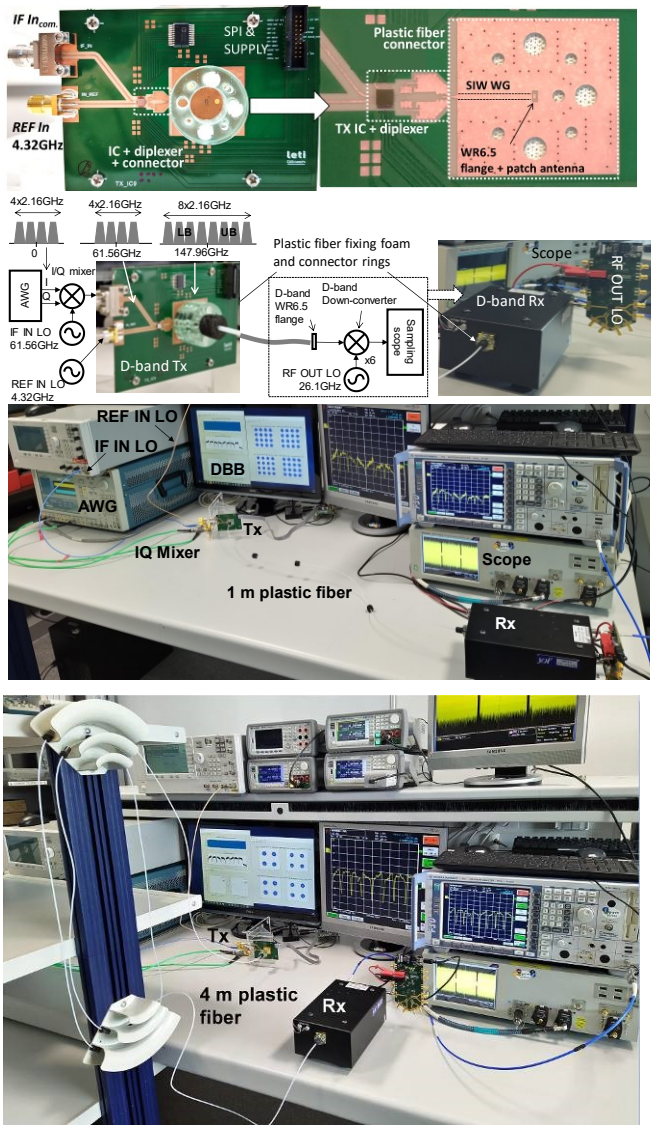

Fig. 11 Transmiter module and 1m and 4m plastic waveguide links.

IV. Conclusions

Increasing the data rate of wireless or wired links has been a driving force for developing new architectures and technologies during the last decades. The current trend towards 100 Gb/s and higher data-rates has brought interest to frequencies beyond 100 GHz where enough BW is available to carry such high data-rates. In this context, the channel bonding architecture discussed in this paper offers an interesting approach to cope with the specific characteristics in terms of propagation and power consumption that appear at this frequency range. The D-band wireless link described in this work achieves one of the lowest energy consumption reported while providing a very high-data rate paving the way to CMOS based 100 Gb/s, meter range point-to-point communications. The same architecture applied to plastic waveguide links achieves the highest data-rates compared with prior works as shown in Fig. 13, with a competitive energy efficiency per unit length of 4 pJ/b/m. These results highlight the interest of channel bonding architectures for high data-rate communications at D-band and sub-THz frequencies.

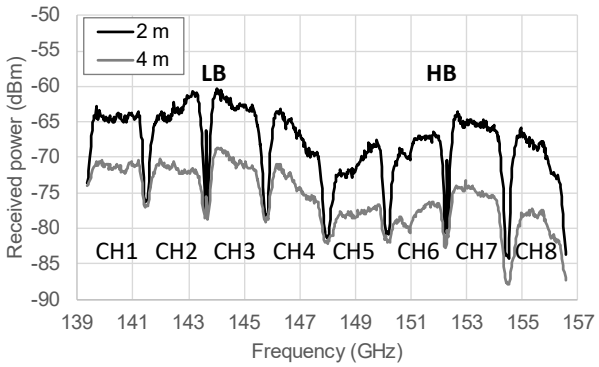

	CH1	CH2	CH3	CH4	CH5	CH6	CH7	CH8
	141.975GHz	144.135GHz	146.295GHz	148.455GHz	150.705GHz	152.865GHz	155.025GHz	157.185GHz
	1.76Gbauds	1.76Gbauds	1.76Gbauds	1.76Gbauds	1.76Gbauds	1.76Gbauds	1.76Gbauds	1.76Gbauds
2 m link	EVM=12.6%	EVM=11.7%	EVM=14.8%	EVM=13.2%	EVM=15.8%	EVM=12.8%	EVM=14.9%	EVM=15.3%
	7.04Gb/s	7.04Gb/s	7.04Gb/s	7.04Gb/s	7.04Gb/s	7.04Gb/s	7.04Gb/s	7.04Gb/s
4 m link	EVM=16.5%	EVM=16.0%	EVM=24.2%	EVM=18.6%	EVM=21.3%	EVM=25.2%	EVM=27.2%	EVM=30.4%
	7.04Gb/s	7.04Gb/s	3.52Gb/s	7.04Gb/s	3.52Gb/s	3.52Gb/s	3.52Gb/s	3.52Gb/s

Fig. 12 Characterization of the modulated signals transmitted through the plastic fiber link at a distance of 2 m and 4 m.

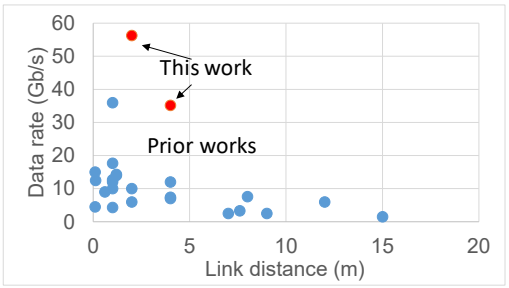

Fig. 13 Comparison of the plastic waveguide link data-rates of this work with previous works.

References

[1] K. K. Tokgoz and K. Okada, "Millimeter-Wave CMOS Transceiver Toward 1Tbps Wireless Communication," in *2019 IEEE International Symposium on Circuits and Systems*, 2019, pp. 1-4.

[2] B. Murmann, "ADC Performance Survey 1997-2021," [Online]. Available: http://web.stanford.edu/~murmann/adcsurvey.html

[3] A. Dascurcu, *et al*, "A 60GHz Phased Array Transceiver Chipset in 45nm RF SOI Featuring Channel Aggregation Using HRM-Based Frequency Interleaving," in *IEEE Radio Frequency Integrated Circuits Symposium (RFIC)*, June 2022, pp. 67-70.

[4] A. Hamani, *et al*. "A 84.48-Gb/s 64-QAM CMOS D-band channel-bonding Tx front-end with integrated multi-LO frequency generation," *IEEE Solid-State Circuits Letters,* vol. 3, pp. 346-349, 2020

[5] A. Hamani, *et al*., "A D-Band Multichannel TX System-in-Package Achieving 84.48 Gb/s With 64-QAM Based on 45-nm CMOS and Low-Cost PCB Technology," in *IEEE Transactions on Microwave Theory and Techniques*, vol. 70, no. 7, pp. 3385-3395, July 2022.

[6] A. Hamani, *et al*., "A 56.32Gb/s 16-QAM D-Band Wireless Link Using RX-TX Systems-in-Package with Integrated Multi-LO Generators in 45nm RFSOI," in *IEEE Radio Frequency Integrated Circuits Symposium (RFIC)*, June 2022, pp. 75-78.

[7] A. Siligaris *et al.*, "A Multichannel Programmable High Order Frequency Multiplier for Channel Bonding and Full Duplex Transceivers at 60 GHz Band," in *IEEE Radio Frequency Integrated Circuits Symposium (RFIC)*, 2020, pp. 259-262.

[8] J. L. Gonzalez-Jimenez *et al*., "A 56.32 Gb/s 16-QAM Link over Dielectric Fiber using a D-band Channel Bonding Transceiver," in *51st European Microwave Conference (EuMC)*, 2022, pp. 197-200.